10.1098/rspa.2000.0581

THE ROYAL SOCIETY

Kinematic dynamo action in a sphere II. Symmetry selection

By David Gubbins, C. N. Barber, S. Gibbons† and J. J. Love

Department of Earth Sciences, University of Leeds, Leeds LS2 9JT, UK

Received 16 July 1999; revised 8 November 1999; accepted 18 November 1999

The magnetic fields of the planets are generated by dynamo action in their electrically conducting interiors. The Earth possesses an axial dipole magnetic field but other planets have other configurations: Uranus has an equatorial dipole for example. In a previous paper we explored a two-parameter class of flows, comprising convection rolls, differential rotation (D) and meridional circulation (M), for dynamo generation of steady fields with axial dipole symmetry by solving the kinematic dynamo equations. In this paper we explore generation of the remaining three allowed symmetries: axial quadrupole, equatorial dipole and equatorial quadrupole. The results have implications for the fully nonlinear dynamical dynamo because the flows qualitatively resemble those driven by thermal convection in a rotating sphere, and the symmetries define separable solutions of the nonlinear equations.

Axial dipole solutions are generally preferred (they have lower critical magnetic Reynolds number) for $D > 0$, corresponding to westward surface drift. Axial quadrupoles are preferred for $D < 0$, and equatorial dipoles for convection with little D or M. No equatorial quadrupole solutions have been found. Symmetry selection can be understood if one assumes that the flow concentrates flux in certain places without reference to sign. Fields with dipole symmetry must change sign across the Equator; if flux is concentrated at the Equator, as tends to be the case for $D < 0$, they have a small length-scale and consequent high dissipation, making them harder to generate than axial quadrupoles. If flux is concentrated nearer the poles ($D > 0$), axial dipoles are preferred. The equatorial dipole must change sign between east and west hemispheres, and is not favoured by any elongation of the flux in longitude (caused by D) or polar concentrations (caused by M): they are preferred for small D and M. Polar and equatorial concentrations can be related to dynamo waves and the sign of Parker's dynamo number. For the three-dimensional flow considered here, the sign of the dynamo number is related to the sense of spiralling of the convection rolls, which must be the same as the surface drift.

Keywords: kinematic dynamo; geomagnetism; symmetry

1. Introduction

Planetary magnetic fields are generated by dynamo action in their fluid electrically conducting interiors (Jacobs 1987; Proctor & Gilbert 1994; Proctor *et al.* 1993; Hollerbach 1996; Fearn 1998). In the kinematic dynamo problem the fluid flow is

† Present address: School of Mathematical Sciences, University of Exeter, Exeter EX4 4QJ, UK.

fixed and Maxwell's equations are solved for a growing magnetic field (Moffatt 1978). Numerical solutions in a sphere can be used to test a flow for dynamo action and to relate the morphology of the generated magnetic field to the fluid flow. Two important questions can therefore be addressed by the kinematics: (*a*) what aspects of the flow cause field generation? and (*b*) what causes the field to have its observed character?

The Earth has possessed a magnetic field approximating an axial dipole for most of its history; Mercury, Jupiter and Saturn have axial dipole magnetic fields today, while Uranus and Neptune have non-axial configurations. In its most basic form, question (*b*) amounts to determining the preferred symmetry of solutions to the kinematic dynamo problem. In a previous paper (Gubbins *et al*. 2000, hereafter referred to as paper I) we explored generation of axial dipole magnetic fields by a two-parameter class of flows. In this paper we explore generation of the remaining three possible symmetries by the same class of flows.

Kumar & Roberts (1975) studied flows defined by the equation

$$\boldsymbol{v} = \epsilon_0 \boldsymbol{t}_1^0 + \epsilon_1 \boldsymbol{s}_2^0 + \epsilon_2 \boldsymbol{s}_2^{2c} + \epsilon_3 \boldsymbol{s}_2^{2s}, \tag{1.1}$$

where $\boldsymbol{t}_l^m$, $\boldsymbol{s}_l^m$ are toroidal and poloidal vector spherical harmonics. The first harmonic represents differential rotation, the second meridional circulation, and the last two represent convective overturn, all of which are likely to occur in a convecting rotating sphere. In paper I we scaled the flow to unit energy, set $\epsilon_2 = \epsilon_3$ and parametrized the flow with the fraction of energy in the meridional circulation, M, and in differential rotation, D; these define a diamond $|D + M| < 1$ in parameter space. Kumar & Roberts (1975) restricted their study close to the point $D = 1$, where the induction equation can be approximated by a mean field equation derived originally by Braginsky (1964). We refer to the points $D = \pm 1$ as Braginsky limit points, where many solutions have been found.

The magnetic field satisfies the induction equation:

$$\frac{\partial \boldsymbol{B}}{\partial t} = R_{\mathrm{m}} \nabla \times (\boldsymbol{v} \times \boldsymbol{B}) + \nabla^2 \boldsymbol{B}, \tag{1.2}$$

where R_{m} is the dimensionless magnetic Reynolds number, and the solenoidal condition

$$\nabla \cdot \boldsymbol{B} = 0. \tag{1.3}$$

Solutions have the form $\boldsymbol{B} = \hat{\boldsymbol{B}} \exp(\sigma + \mathrm{i}\omega)t$. $\hat{\boldsymbol{B}}$ satisfies the eigenvalue equation

$$(\sigma + \mathrm{i}\omega)\hat{\boldsymbol{B}} = R_{\mathrm{m}} \nabla \times (\boldsymbol{v} \times \hat{\boldsymbol{B}}) + \nabla^2 \hat{\boldsymbol{B}}. \tag{1.4}$$

Dynamo action is said to occur when a growing solution exists with $\sigma \geqslant 0$; the critical magnetic Reynolds number $R_{\mathrm{m}}^{\mathrm{c}}$ is the value corresponding to marginal stability or overstability with $\sigma = 0$. When more than one solution is found, the one with smaller $R_{\mathrm{m}}^{\mathrm{c}}$ is the most unstable and is usually referred to as physically realizable. However, the solution to the corresponding nonlinear problem may relate to several linear modes, making them all physically interesting (Jennings & Weiss (1991) and Grote *et al*. (2000), for example, both find nonlinear solutions with mixed dipole–quadrupole symmetry, but in the linear kinematic problem these symmetries are linearly independent). Equation (1.4) is solved numerically in a sphere subject to insulating boundary conditions using the numerical procedure detailed in paper I.

The flow defined by equation (1.1) is invariant under reflection in the equatorial plane (E) and rotation by an angle π about the polar axis (P), which follows because $\boldsymbol{v}$ contains only azimuthal modes $\mathrm{e}^{\mathrm{i}m\phi}$ with $m = 0$ and 2. $\boldsymbol{v}$ forms a coefficient in equation (1.4), which is linear in $\boldsymbol{B}$, and therefore solutions decouple into four sets in which $\boldsymbol{B}$ remains invariant or changes sign under transformations E and P. The Earth's magnetic field exhibits both these symmetries to some extent: the dipole and some smaller features are antisymmetric about the Equator, while departures from axial symmetry tend to lie on the same longitudes 120–180° apart (Bloxham & Gubbins 1985). The four possible symmetries are $E^{\mathrm{A}}P^{\mathrm{S}}, E^{\mathrm{S}}P^{\mathrm{S}}, E^{\mathrm{S}}P^{\mathrm{A}}$ and $E^{\mathrm{A}}P^{\mathrm{A}}$, where S, A refer to symmetric, antisymmetric. We adopt Holme's (1997) more concise notation $D_{\mathrm{a}}, Q_{\mathrm{a}}, D_{\mathrm{e}}, Q_{\mathrm{e}}$ where D, Q denote dipole, quadrupole, and subscripts a, e denote axial, equatorial. The symmetry properties arise ultimately because of the geometry of a rotating sphere and rotational invariance of Maxwell's equations and the Lorentz transformation in the non-relativistic limit (Gubbins & Zhang 1993). Equation (1.2) is linear in $\boldsymbol{B}$ and solutions with different symmetries are independent. However, these solutions are also separable for the full nonlinear dynamo problem; the kinematic results are therefore relevant for dynamical studies.

The adjoint to the induction equation is formed by changing the sign of R_{m} and the boundary conditions (Gibson & Roberts 1966; Kono & Roberts 1991). Eigensolutions to the adjoint equation have the same critical magnetic Reynolds number (eigenvalue) but different symmetry (Proctor 1977*b*). This property can help us find new dynamo solutions: having found a dynamo at R_{m} we can search for another at $-R_{\mathrm{m}}$ with different symmetry. The boundary conditions of the adjoint problem are unphysical, but for some flows the boundary conditions are rather unimportant and may be replaced by the physical boundary conditions (Proctor 1977*a*). Hutcheson & Gubbins (1994) found numerical demonstrations of the adjoint symmetry by surrounding the spherical dynamo region by a large sphere of stagnant fluid, thus approximating boundaries at infinity. Then, by reducing the size of the surrounding shell, they found numerical solutions to the physical problem with opposite symmetry near $-R_{\mathrm{m}}$. Changing the sign of R_{m} is equivalent to changing the signs of both D and M, or inversion through the origin of parameter space. For example, if boundary conditions were completely unimportant the plot of $R_{\mathrm{m}}^{\mathrm{c}}$ for the axial quadrupole solutions would appear as the plot of $R_{\mathrm{m}}^{\mathrm{c}}$ for the axial dipole solutions inverted through the origin.

Sarson & Gubbins (1996) found Q_{a} solutions near the Braginsky limit $D \to -1$, corresponding to quadrupole solutions of the mean field equations. Holme (1997) reported a D_{e} solution for $M = D = 0$. These are the only dynamos found so far for fields with D_{e} or Q symmetry. Holme (1997) searched mainly for D_{e} solutions on the boundary of our square $|D + M| = 1$, where the flow is axisymmetric and solutions proportional to $\exp(\mathrm{i}m\phi)$ separate. He found none, and we have not searched the boundary (he did succeed in finding D_{e} solutions on the boundary, and a single Q_{a} solution, with a slight modification of the flow).

2. Steady solutions

(*a*) *Axial quadrupole solutions*

We have examined flows on a 0.05×0.05 grid in D, M parameter space. Most dynamos were found to be steady, as was the case for the axial dipole solutions. We found

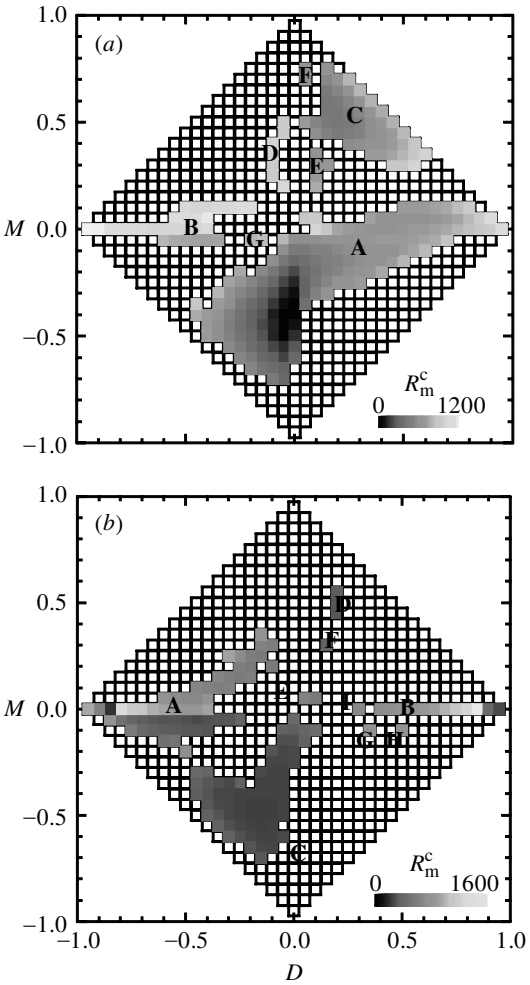

Figure 1. R_m^c for flows generating (*a*) axial dipole fields, from paper I, and (*b*) axial quadrupole fields. Logarithmic scale.

145 grid squares defining velocities that generate Q_a fields, representing *ca.* 19% of all possible flows. The critical magnetic Reynolds numbers are plotted in figure 1 alongside the D_a solutions from paper I. Dynamo action occurs in discrete zones of parameter space separated by regions where no dynamo action appears to occur, as for the D_a solutions. Zones A, B, C of the quadrupole solutions correspond roughly to A, B, C of the dipole solutions, as anticipated from the adjoint symmetry. The other zones are too dissimilar to make any such association. R_m^c is smallest in zone C and the lower part of zone A; the range is broadly similar to that for the axial dipole solutions.

Figure 2*a* shows the ohmic heating normalized to unit energy. It is an alternative gauge of the efficiency of the dynamo, a low value indicating low dissipation. The plot is similar to that for R_m^c except for the Braginsky limit points, where a large R_m^c is required to generate a large-scale toroidal field with relatively little dissipation. As for the D_a solutions, differential rotation promotes toroidal field and meridional

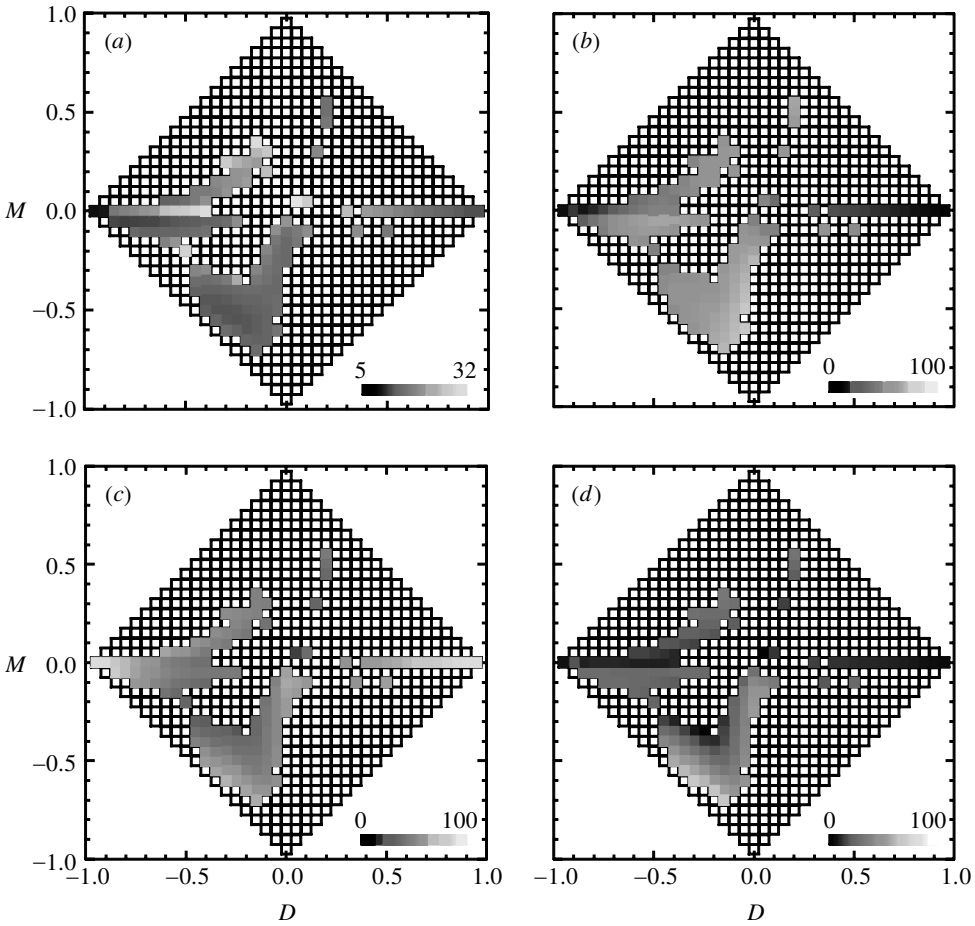

Figure 2. Physical properties of the axial quadrupole solutions: (*a*) ohmic heating divided by magnetic energy (this is a thermodynamic measure of the 'efficiency' of the dynamo); (*b*) percentage energy in the poloidal field; (*c*) percentage energy in the axisymmetric part of the field; (*d*) percentage of poloidal energy that is axisymmetric.

circulation promotes poloidal field; both tend to promote axisymmetric fields. Figure 2*b* shows the percentage of energy in the poloidal magnetic field. Regions A and B are dominated by toroidal energy; there is a roughly equal partition of poloidal and toroidal energy near the centre of the diamond; and the maximum poloidal energy occurs in region C with weak differential rotation. Figure 2*c* shows the percentage of axisymmetric energy, which generally increases with both $|D|$ and $|M|$. Figure 2*d* shows the percentage of axisymmetric energy in the poloidal field; the Braginsky limit points are low because the poloidal non-axisymmetric field dominates in the limit.

The flow $D = -0.50$, $M = -0.05$ in zone A generates a fairly simple field shown in figure 3*a*. The surface flux is concentrated at the poles and in two patches on the Equator; large departures from axial symmetry in the poloidal field make $\boldsymbol{S}_2^2$ the dominant harmonic, as it is for most Q_{a} dynamos. The toroidal field comprises equatorial rings (figure 3*b*), with dominant harmonic $\boldsymbol{T}_1^0$. Solutions throughout zone A

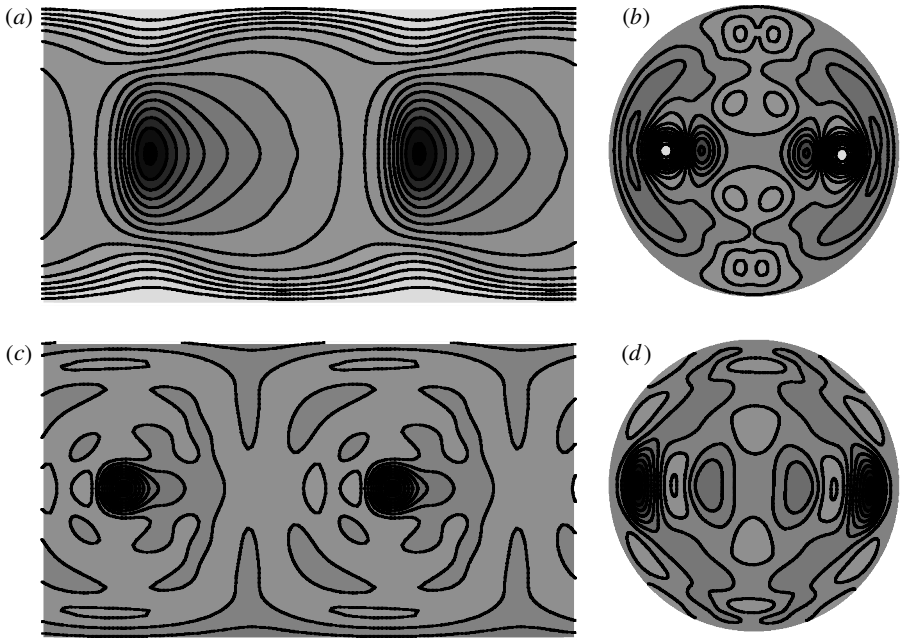

Figure 3. Q_{a} magnetic field generated by flow in zone A of figure 1*b*, showing change of field with change of sign of M: (*a*) $D = -0.50$, $M = -0.05$, $R_{\mathrm{m}}^{\mathrm{c}} = 78$, B_r on surface; (*b*) B_ϕ in meridian section, $\phi = 0$; (*c*) $D = -0.50$, $M = 0.05$, $R_{\mathrm{m}}^{\mathrm{c}} = 270$, B_r on surface; (*d*) B_ϕ in meridian section, $\phi = 0$.

can be understood in terms of the effects of D and M on this solution. Increasing M to zero and positive values eliminates the polar flux and concentrates the equatorial spots (figure 3*c*). Decreasing D towards the Braginsky limit $D = -1$ increases the toroidal field; with $M < 0$ it eliminates the equatorial poloidal spots and with $M \geqslant 0$ elongates them in longitude (see figure 9*c*). At the other Braginsky limit ($D = 1$ in zone B) the poloidal field is also concentrated onto the Equator but with some latitudinal structure; the dominant toroidal harmonic is $\boldsymbol{T}_3^0$.

Zone C is the largest and contains the dynamos with smallest $R_{\mathrm{m}}^{\mathrm{c}}$. Solutions for $D < 0$ and moderate M resemble those in neighbouring zone A; the dominant harmonics are $\boldsymbol{S}_2^2$ and $\boldsymbol{T}_1^0$. The solution for $D = -0.10$, $M = -0.55$ has one of the smallest values of $R_{\mathrm{m}}^{\mathrm{c}}$; the field is shown in figures 4*a*, *b*. Throughout this zone meridional circulation sweeps surface flux towards the poles, promoting axisymmetric fields, and internal toroidal flux towards the Equator. Solutions with $D \geqslant 0$ are somewhat different in having toroidal field distributed throughout the sphere (figure 4*c*); the dominant harmonic is $\boldsymbol{T}_3^0$ (as is found throughout neighbouring zone B).

Zones D and F have low $R_{\mathrm{m}}^{\mathrm{c}}$ but strong departures from axial symmetry. The surface field alternates in sign around the Equator (figure 4*d*). The remaining small zones have large $R_{\mathrm{m}}^{\mathrm{c}}$ and small-scale magnetic fields.

(*b*) *Equatorial dipole solutions*

Equatorial dipole solutions, D_{e}, have been found in 68 grid squares or 9% of the flows. Like the two previous symmetries, they lie in discrete zones in parameter space,

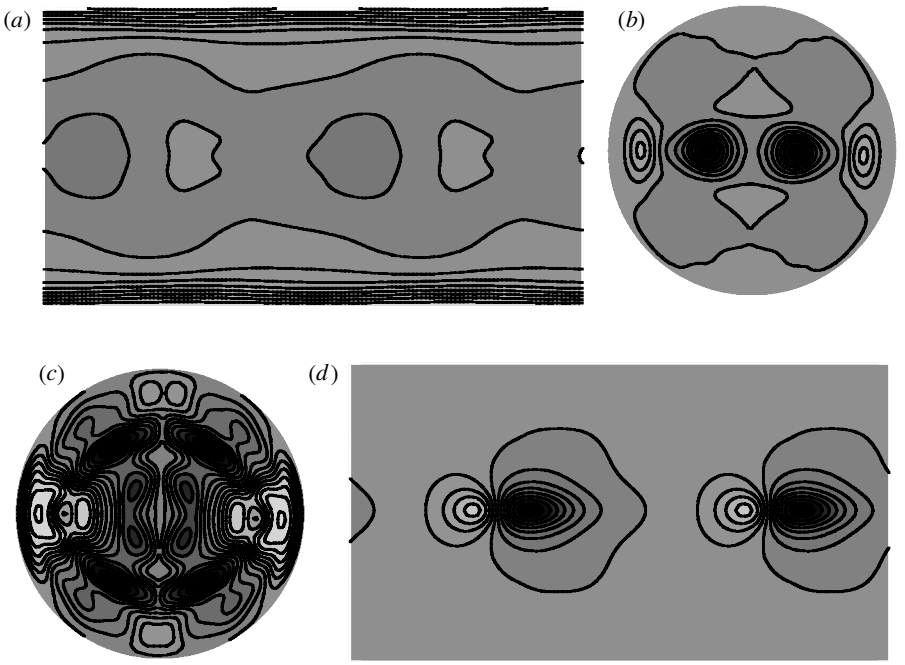

Figure 4. Magnetic field generated by flow in zone C: (*a*) $D = -0.10$, $M = -0.55$, $R_{\rm m}^{\rm c} = 54$, B_r on surface; (*b*) B_ϕ in meridian section, $\phi = 0$; (*c*) $D = 0.00$, $M = -0.10$, B_ϕ, zone C showing toroidal flux distributed throughout the sphere; (*d*) $D = 0.20$, $M = 0.45$, zone D, B_r at surface.

labelled A–E in figure 5*a*. The leading harmonics in the spherical harmonic expansion of this symmetry are $\boldsymbol{S}_1^1$ and $\boldsymbol{T}_2^1$, and these generally contain the most energy. The main zones, A and B, have the lowest $R_{\rm m}^{\rm c}$ and simplest field configurations; $R_{\rm m}^{\rm c}$ is much higher in the three smaller zones. The poloidal energy (figure 5*b*) is highest in region B and near the centre of the plot. As expected, M generally promotes poloidal field while D promotes toroidal field. Zone D is an exception, being dominated by toroidal flux with harmonic $\boldsymbol{T}_4^1$. The ohmic heating (figure 5*c*) follows the plot of $R_{\rm m}^{\rm c}$ as expected. It is generally higher than for either axial symmetry.

The solution at the very centre of the sphere was found by Holme (1997). The field is shown in figure 6; it is large scale and dominated by an equatorial dipole. The field generated by neighbouring flows in zone B is simpler still, with slightly smaller $R_{\rm m}^{\rm c}$. Increasingly negative D stretches the regions of flux in longitude; M spreads them in latitude. Fields in zone A are similar, but increasing M squashes the flux onto the Equator. Zone C has field concentrated into very small patches on the Equator. Zone D is similar, but the surface flux has a positive and negative series of flux patches around the Equator, rather like the $Q_{\rm a}$ solutions in zones D and F (see figure 4*d*). Zone E has surface flux elongated in latitude and a very complex small scale B_ϕ.

3. Overlapping solutions

Many flows sustain dynamos with two or even three symmetries (table 1). The solution with lowest $R_{\rm m}^{\rm c}$ is displayed in figure 7; these are the physically realizable solu-

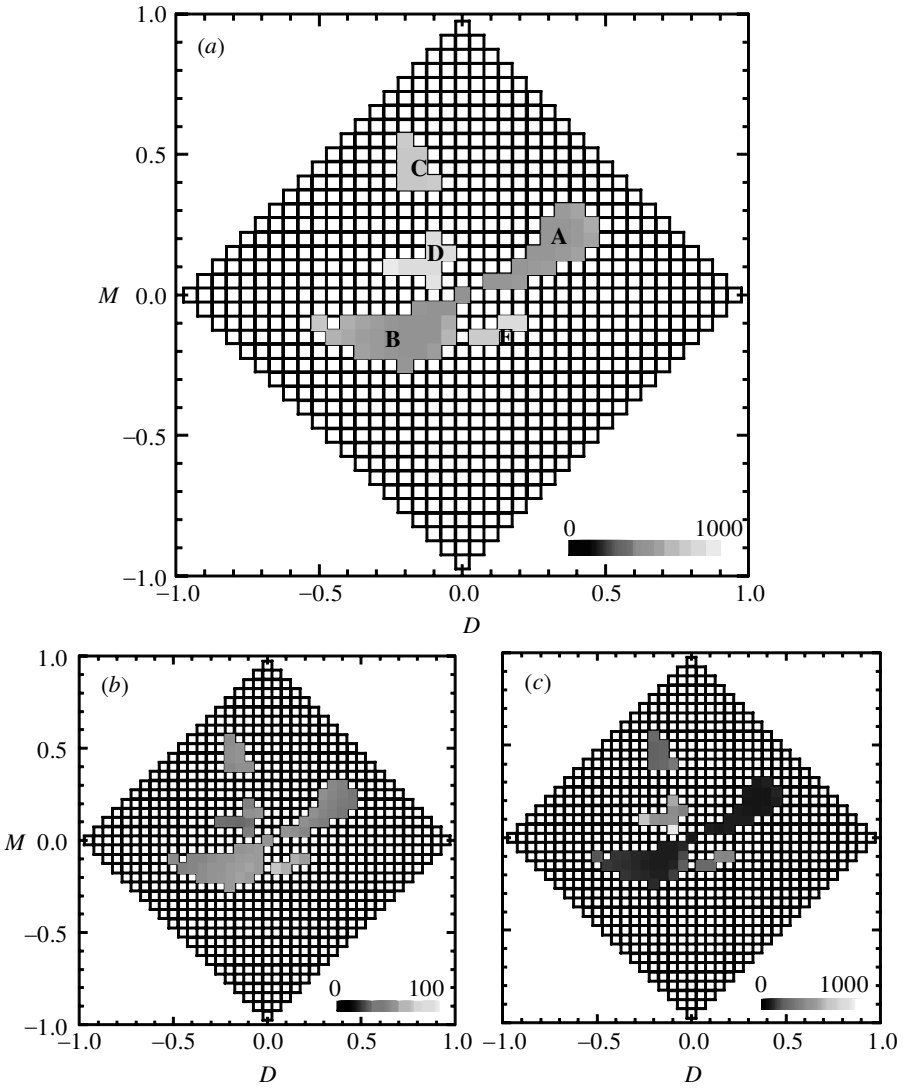

Figure 5. Physical properties of the equatorial dipole solutions: (*a*) critical magnetic Reynolds numbers of the equatorial dipole solutions in distinct regions A–E; (*b*) percentage energy in the poloidal field, equatorial dipole solutions; (*c*) ohmic heating divided by magnetic energy of the equatorial dipole solutions.

tions. The amount of overlap can be judged by comparing the separate diamonds for each symmetry (figures 1*a*, *b* and 5*a*).

The most striking result is the preference for D_{a} solutions when $D > 0$, Q_{a} solutions when $D < 0$ and D_{e} solutions near the centre of the diamond when $DM > 0$.

$R_{\mathrm{m}}^{\mathrm{c}}$ on two squares in figure 7, $D = -0.90, -0.95$, $M = 0.00$, are radically different to what one would expect. This is because the Q_{a} solutions are oscillatory there (see Sarson & Gubbins (1996) for other examples) and the steady D_{a} solution, which has smaller $R_{\mathrm{m}}^{\mathrm{c}}$, is represented. The oscillatory solutions are confined to a very narrow

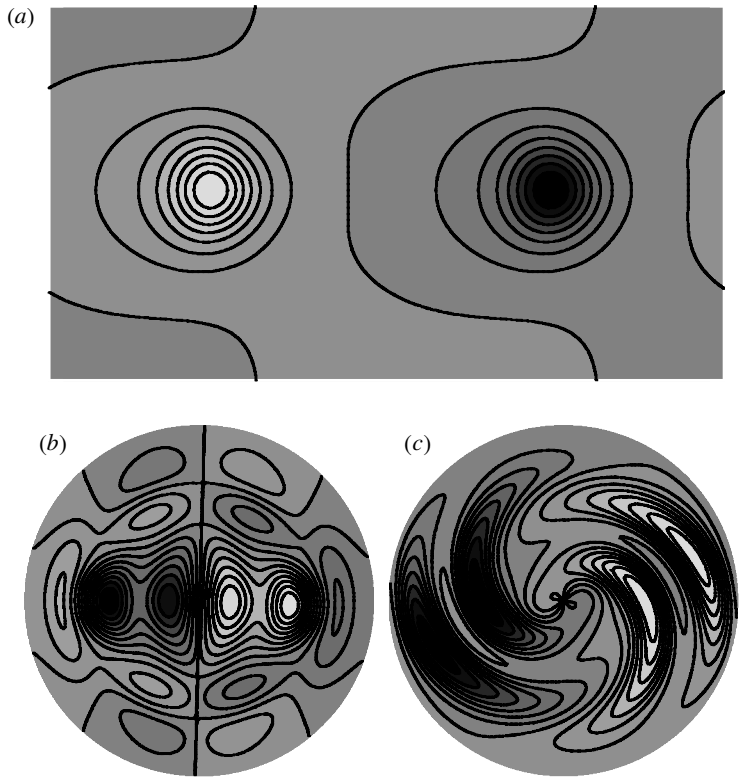

Figure 6. Equatorial dipole magnetic field generated by flow $D = 0.00$, $M = 0.00$, $R_{\mathrm{m}}^{\mathrm{c}} = 41$, typical of zones A and B: (*a*) B_r on surface; (*b*) B_r in meridian section, $\phi = 0$; (*c*) B_ϕ in equatorial section.

Table 1. *Statistics of solutions of the three symmetries found*

(The second column gives the percentage of squares where only that combination of solutions is found; the third column gives the percentage generating at least those symmetries.)

solutions	exclusive (%)	total (%)	lowest $R_{\mathrm{m}}^{\mathrm{c}}$ (%)
D_{a}	20.2	36.0	27.7
Q_{a}	4.5	19.1	12.1
$D_{\mathrm{a}} + Q_{\mathrm{a}}$	13.5	14.2	
D_{e}	6.4	9.1	8.0
$D_{\mathrm{a}} + D_{\mathrm{e}}$	1.6	3.8	
$Q_{\mathrm{a}} + D_{\mathrm{e}}$	0.4	1.1	
$D_{\mathrm{a}} + Q_{\mathrm{a}} + D_{\mathrm{e}}$	0.7	0.7	

range of M and the vast majority of Q_{a} solutions in this region are steady with much lower $R_{\mathrm{m}}^{\mathrm{c}}$ than the D_{a} solutions. Similar behaviour occurs near the other Braginsky limit point $D = 1$, where preferred dipole solutions become oscillatory. The oscillatory solutions will be discussed in a third paper of this series.

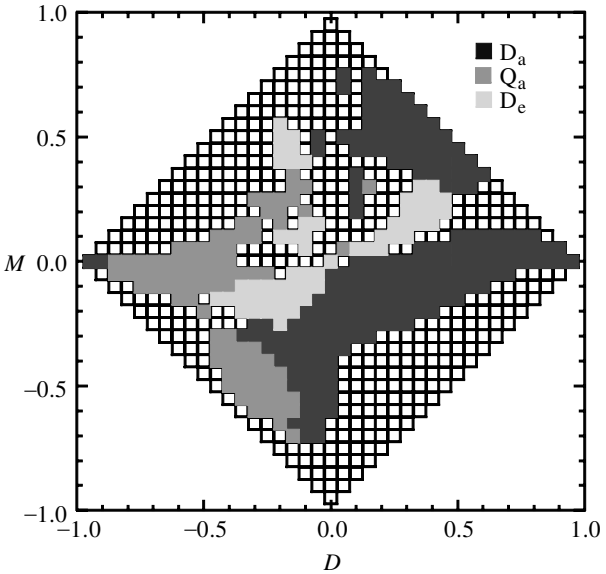

Figure 7. Symmetry of solution with the lowest $R_{\mathrm{m}}^{\mathrm{c}}$. Some flows generate more than one symmetry (cf. figures 1, 5*a*). D_{a} and Q_{a} solutions have the same $R_{\mathrm{m}}^{\mathrm{c}}$ along the boundary indicated; this does not happen on other boundaries.

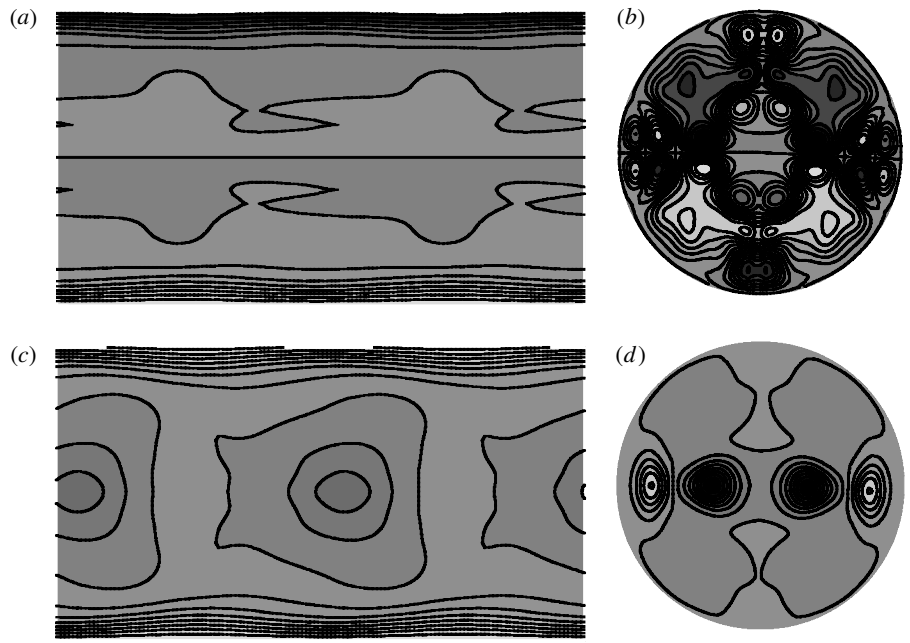

Figure 8. Magnetic field solutions for $D = -0.15$, $M = -0.50$: (*a*) B_r at surface, D_{a} solution ($R_{\mathrm{m}}^{\mathrm{c}} = 50$); (*b*) B_ϕ in meridian section, $\phi = 0$, D_{a}; (*c*) B_r, Q_{a} solution ($R_{\mathrm{m}}^{\mathrm{c}} = 51$); (*d*) B_ϕ, Q_{a}.

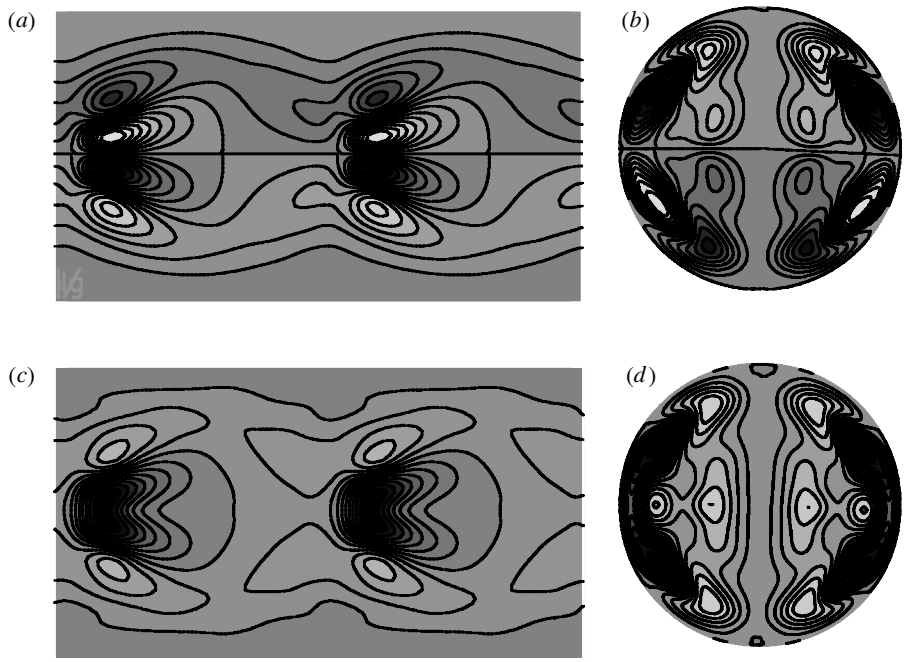

Figure 9. Magnetic field solutions for $D = -0.85$, $M = 0.00$: (*a*) B_r, D_a solution ($R_\mathrm{m}^\mathrm{c} = 812$); (*b*) B_ϕ, D_a; (*c*) B_r, Q_a solution ($R_\mathrm{m}^\mathrm{c} = 801$); (*d*) B_ϕ, Q_a.

The main overlap is between D_a and Q_a, and flows defined by a line in the diamond running from about $D, M = -0.20, -0.65$ up to $-0.25, -0.40$ in figure 7 generate both D_a and Q_a fields at the same R_m^c. Figure 8 shows the fields for the pair of solutions for one point on this line. The toroidal fields are concentrated near the Equator; for Q_a they are relatively simple, while for D_a they are much more complex, partly because the symmetry forces it to change sign across the Equator. This explains why Q_a solutions are preferred to the left of this line: the larger differential rotation generates a stronger toroidal field, the smaller scale of the D_a solution involves higher dissipation and therefore needs a higher R_m^c. Poloidal flux is polar; the D_a solution has a simple pair of flux concentrations of opposite sign, but the Q_a symmetry forces the field to reverse elsewhere, giving it a smaller length-scale. The poloidal field, therefore, has lower dissipation for the D_a mode. This explains why D_a solutions are preferred to the right of this line.

A similar argument applies to solutions near the Braginsky limit points, $D = \pm 1$, both of which support both D_a and Q_a solutions. Near $D = -1$, both poloidal and toroidal flux are concentrated near the Equator, and Q_a is preferred (figure 9). Near $D = 1$ the solutions have radically different R_m^c and magnetic fields, and the D_a solution is preferred.

D_a and D_e solutions have less overlap and the solutions are quite different. For example, for purely poloidal flows $M = -0.05$ supports D_a but not D_e, while $M = 0$ supports only D_e. Both solutions are supported at $M = -0.02$, and we display them for comparison in figure 10; the flux is concentrated onto the Equator, where the D_a solution must change sign and reduce its length-scale relative to D_e. The D_e solution changes sign with longitude, reducing its length-scale relative to D_a. Decreasing M

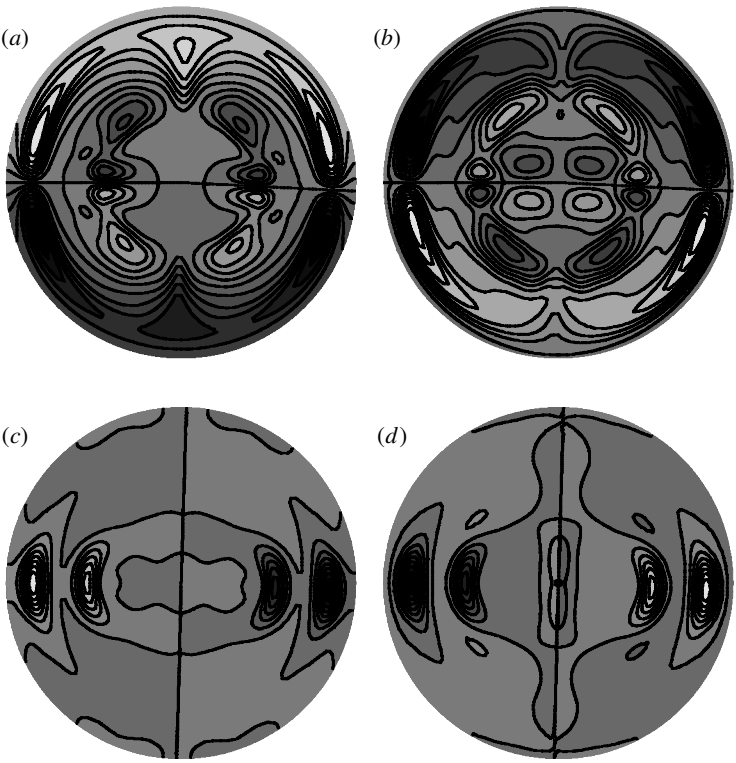

Figure 10. $D_{\rm e}$ ($R_{\rm m}^{\rm c} = 179$) and $D_{\rm a}$ ($R_{\rm m}^{\rm c} = 131$) solutions compared at $D = 0.00$, $M = -0.02$: (*a*) $D_{\rm a}$, B_r in meridian section, $\phi = 90°$; (*b*) $D_{\rm a}$, B_ϕ; (*c*) $D_{\rm e}$, B_r; (*d*) $D_{\rm e}$, B_ϕ.

moves flux towards the poles, promoting axially symmetric field and favouring the $D_{\rm a}$ symmetry as observed.

There are only three squares generating both $D_{\rm e}$ and $Q_{\rm a}$ fields. As with flows generating both $D_{\rm a}$ and $Q_{\rm a}$ solutions, flux tends to be generated in the same place with the symmetry forcing sign changes, but in this case between east and west rather than north and south. $D = -0.40, M = -0.10$ is a nice example (figure 11) with poloidal flux concentrated at the poles and Equator, and toroidal flux at the Equator only.

A cluster of flows around $D = -0.10$, $M = -0.20$ generates all three symmetries with similar $R_{\rm m}^{\rm c}$. When all three symmetries are generated the surface $D_{\rm a}$ field has the double clover leaf pattern (fig. 6*a* of paper I). Because of their symmetry all solutions have flux that is forced to change sign over a short distance.

4. Discussion

We have established that almost half of the flows defined by equation (1.1) generate a steady magnetic field with at least one of the possible symmetries. Axial dipoles are the most commonly excited, followed by axial quadrupoles, then equatorial dipoles, and no equatorial quadrupoles have been found. Some of this ordering arises from the spatial complexity, and concomitant ohmic dissipation, of the different symmetries. The leading poloidal harmonics are $\boldsymbol{S}_1^0$ for the $D_{\rm a}$ fields and $\boldsymbol{S}_2^0$ for the $Q_{\rm a}$; $D_{\rm a}$

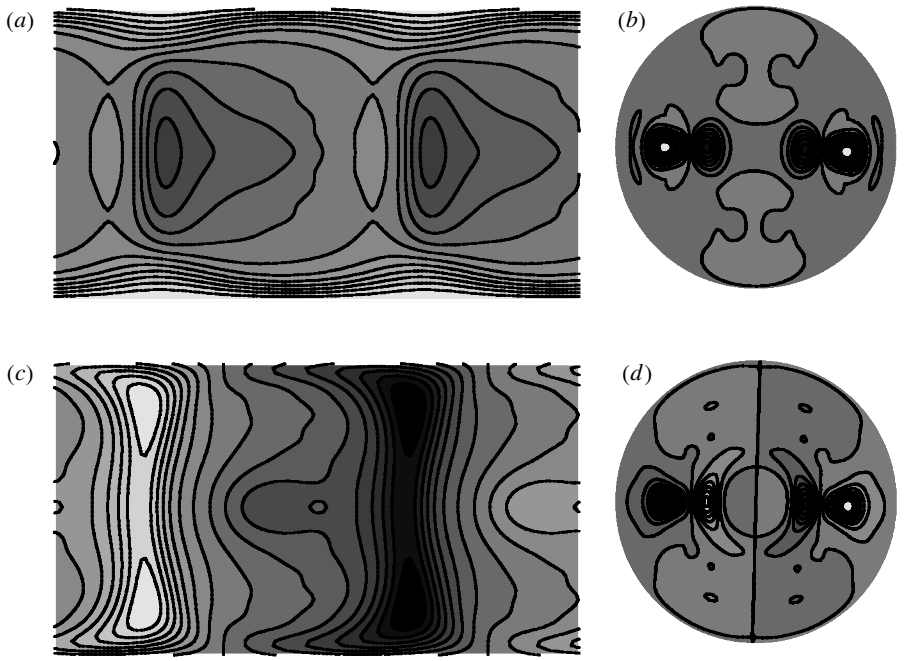

Figure 11. Magnetic field solutions for $D = -0.40$, $M = -0.10$: (*a*) B_r, Q_a solution ($R_\mathrm{m}^\mathrm{c} = 80$); (*b*) B_ϕ, Q_a; (*c*) B_r, D_e solution ($R_\mathrm{m}^\mathrm{c} = 100$); (*d*) B_ϕ, D_e.

fields can therefore be expected to have lower dissipation in a dynamo solution. Furthermore, if the toroidal field is generated by differential rotation acting on the poloidal field, Q_a solutions will have a substantial $\boldsymbol{T}_3^0$ component, which is of higher degree than the dominant $\boldsymbol{T}_2^0$ harmonic of the D_a fields, even though the leading harmonic is $\boldsymbol{T}_1^0$.

This argument does not apply to the D_e solutions, whose poloidal fields have similar complexity to D_a. We found that D and M both promote axisymmetric flux for axial solutions, but D_e has no axisymmetric component: it is therefore not surprising that the solution with $D = M = 0$ is lost when these parameters are increased. Love & Gubbins (1996) attributed failure of the $D = M = 0$ flow to generate D_a fields to uniform distortion of the magnetic field lines by the axisymmetric helicity, which leads to cancellation rather than reinforcement of the pre-existing field. However, the D_e fields vary with $\cos\phi$ or $\sin\phi$ and the distortion of uniform helicity will therefore produce a non-axisymmetric field capable of reinforcement. Dynamo action is lost when $|M|$ departs slightly from zero, perhaps because of the action of non-axisymmetric helicity.

The failure of the axisymmetric flows on the boundary $|D+M| = 1$ to generate D_e fields is surprising. Holme (1997) attributes this to strong shear near the boundary, and obtains dynamo action by changing the radial structure of the flow slightly. This modified flow might well generate a higher proportion of D_e fields in the main body of the diamond.

If one accepts that these flows generate fields preferentially in certain places but without regard to sign, then symmetry selection can be understood in terms of the spatial structure imposed on the field. D_a fields must change sign across the Equator,

but Q_a fields do not. However, the solenoidal condition (1.3) demands sign changes somewhere: Q_a fields change sign away from the Equator, while D_e fields change sign in longitude. Thus polar flux favours D_a and equatorial flux Q_a or D_e, depending on the elongation in longitude. Flux concentration is not always so simple. Some flows tend to generate flux in two distinct regions, for example at the poles and the Equator. Others may generate poloidal flux in one region and toroidal flux in another. Different concentrations can favour different symmetries, making it difficult or impossible to predict a preference. This is the case along the boundary between D_a and Q_a solutions in figure 7 ($D < 0$, $M < 0$), where a line of flows have identical R_m^c for the two symmetries.

The previous discussion begs the question of why the flow should generate strong field in certain places. There is a tendency for the convective part of the flow to generated field along the boundaries of the cells, particularly radial field at the surface where fluid downwells. This could simply be a result of flux expulsion from the core of the convective cell. Parker (1979) explains equatorial or polar concentrations of flux in steady $\alpha\omega$ dynamos in terms of interference of dynamo waves that propagate equatorward for positive 'dynamo number' ($\alpha\omega > 0$) in the Northern Hemisphere (our point $D = -1$), giving steady dynamos with flux concentrated around the Equator, which would favour Q_a steady fields by the argument of the previous paragraph, and poleward propagation for $\alpha\omega < 0$ ($D = 1$) giving polar flux and D_a steady fields. The sign of Parker's dynamo number is determined in the three-dimensional flow by the sense of spiralling of the convection cells relative to the differential rotation. The convection parameters have been chosen so the rolls spiral towards the west. $D > 0$ corresponds to westward drift at the surface, the geophysical case, and negative radial gradient ($\omega' < 0$ in Parker's notation), and so axial dipole solutions are preferred when both are in the same sense (both can be reversed without changing the equations by one of the symmetry conditions given in paper I). The results given here therefore suggest that a field with axial dipole symmetry requires westward spiralling of the rolls. This is opposite to what is found from non-magnetic rapidly rotating convection (Zhang 1992), where convection rolls drift prograde (east) and also spiral to the east. However, this is a viscous effect, and viscosity is negligible in the Earth. Zhang (1995) found that westward spiralling and westward drift arose in convection with an imposed toroidal magnetic field. A proper comparison with Parker's ideas, which are based on $\alpha\omega$ equations, requires a comparison of oscillatory solutions, which are the subject of paper III of this series.

This research was supported by NERC grant GR3/9741. J.J.L. is supported by the Leverhulme Trust. We thank R. Holme, C. Jones, and G. Sarson for helpful discussions.

References

Bloxham, J. & Gubbins, D. 1985 The secular variation of the Earth's magnetic field. *Nature* **317**, 777–781.

Braginsky, S. I. 1964 Kinematic models of the Earth's hydromagnetic dynamo. *Geomagnetism i Aeronomiya* **4**, 732. (Engl. transl. 1964 *Geomagnetism Aeronomy* **4**, 572–583.)

Fearn, D. R. 1998 Hydromagnetic flow in planetary cores. *Rep. Prog. Phys.* **61**, 175–235.

Gibson, R. D. & Roberts, P. H. 1966 Some comments on the theory of homogeneous dynamos. In *Magnetism and the cosmos* (ed. W. Hindmarsh, F. H. Lowes, P. H. Roberts & S. K. Runcorn), pp. 108–120. Edinburgh: Oliver and Boyd.

Grote, E., Busse, F. H. & Tilgner, A. 2000 Regular and chaotic spherical dynamos. *Phys. Earth Planet. Interiors* (In the press.)

Gubbins, D. & Zhang, K. 1993 Symmetry properties of the dynamo equations for paleomagnetism and geomagnetism. *Phys. Earth Planet. Interiors* **75**, 225–241.

Gubbins, D., Barber, C. N., Gibbons, S. & Love, J. J. 2000 Kinematic dynamo action in a sphere. I. Effects of differential rotation and meridional circulation. *Proc. R. Soc. Lond.* A **456**, 1333–1353.

Hollerbach, R. 1996 On the theory of the geodynamo. *Phys. Earth Planet. Interiors* **98**, 163–185.

Holme, R. 1997 Three-dimensional kinematic dynamos with equatorial symmetry: application to the magnetic fields of Uranus and Neptune. *Phys. Earth Planet. Interiors* **102**, 105–122.

Hutcheson, K. A. & Gubbins, D. 1994 Kinematic magnetic field morphology at the core mantle boundary. *Geophys. Jl Interiors* **116**, 304–320.

Jacobs, J. A. 1987 *Geomagnetism*, vol. II. Academic.

Jennings, R. L. & Weiss, N. O. 1991 Symmetry breaking in stellar dynamos. *Mon. Not. R. Astron. Soc.* **252**, 249–260.

Kono, M. & Roberts, P. H. 1991 Small amplitude solutions of the dynamo problem. 1. The adjoint system and its solutions. *J. Geomagn. Geoelectr.* **43**, 839–862.

Kumar, S. & Roberts, P. H. 1975 A three-dimensional kinematic dynamo. *Proc. R. Soc. Lond.* A **344**, 235–238.

Love, J. & Gubbins, D. 1996 Dynamos driven by poloidal flows exist. *Geophys. Res. Lett.* **23**, 857–860.

Moffatt, H. K. 1978 *Magnetic field generation in electrically conducting fluids.* Cambridge University Press.

Parker, E. N. 1979 *Cosmical magnetic fields: their origin and their activity.* Oxford: Clarendon.

Proctor, M. R. E. 1977*a* The role of mean circulation in parity selection by planetary magnetic fields. *Geophys. Astrophys. Fluid Dyn.* **8**, 311–324.

Proctor, M. R. E. 1977*b* On the eigenvalues of kinematic α-effect dynamos. *Astron. Nachr.* **298**, 19–25.

Proctor, M. R. E. & Gilbert, A. D. 1994 *Stellar and planetary dynamos.* Cambridge University Press.

Proctor, M. R. E., Mathews, P. C. & Rucklidge, A. M. 1993 *Solar and planetary dynamos.* Cambridge University Press.

Sarson, G. & Gubbins, D. 1996 Three-dimensional kinematic dynamos dominated by strong differential rotation. *J. Fluid Mech.* **306**, 223–265.

Zhang, K. 1992 Spiralling columnar convection in rapidly rotating spherical fluid shells. *J. Fluid Mech.* **236**, 535–556.

Zhang, K. 1995 Spherical shell rotating convection in the presence of a toroidal magnetic field. *Proc. R. Soc. Lond.* A **448**, 245–268.